

# Tumor Detection by Color Segmentation of PET/CT Liver Images

Neha Bangar<sup>a</sup>, Akash Deep<sup>a</sup>

<sup>a</sup>University Institute of Engineering and Technology, Panjab University,  
Chandigarh, India  
{neha.bangar1@gmail.com, akashdeep@pu.ac.in}

**Abstract**— A wide range of different image modalities for medical imaging are available now-a-days which provide view of internal structures of the human body such as brain, kidney, liver etc. Among these medical image modalities, Ultrasound (US), Magnetic Resonance Imaging (MRI), Computed Tomography (CT), Positron Emission Tomography (PET) and Positron Emission Tomography combined Computed Tomography (PET/CT) imaging has gained importance in research areas. The key problems within medical image analysis techniques are segmentation and shape feature extraction that will be referred to in this paper. Segmentation of grayscale medical images can be difficult since the intensity values between healthy tissue and tumor may be very close. PET/CT provides more accurate measurements of tumor size than is possible with visual assessment alone. In this paper, segmentation method for the detection of liver tumor in PET/CT scans is proposed. The images are denoised using median filter and binary tree quantization clustering algorithm is used for segmentation. Finally ROI selection and shape feature extraction is performed on the selected cluster to quantify the size of the tumor and to check the accuracy of our method with original image and K-means Clustering method.

**Index Terms**— Denoising, Liver segmentation, Binary Tree Quantization Algorithm, K-means Clustering Algorithm, Shape Feature Extraction.

## I. INTRODUCTION

Tumor/ Cancer are the abnormal growth of cells or tissues in the organ. Liver Cancer is a common type of cancer that affects the largest organ in the abdomen, the liver. There are two types of liver cancer namely Primary Liver Cancer and Secondary Liver Cancer. Primary liver cancer is the cancer that originates from the liver itself. This type of liver cancer is also known as hepatocellular carcinoma (HCC) or hepatoma. It is the fifth most frequent cancer form in the world and third leading cause of cancer death. HCC cases mostly occur in Asia and Africa, but its number is increasing rapidly in U.S. and other western countries [1]. Secondary liver cancer is the cancer which originates in other organs but then spreads to liver [2]. Secondary liver cancer is also known as Metastatic liver cancer. Our interest of research is hepatocellular carcinoma, which we will further refer to as liver tumor. According to American Cancer Society [3], men suffer from liver cancer more than women. As per data from the World Health Organization (WHO), less

than 30 cases per 100,000 people worldwide die as a result of liver cancer, with high rates in parts of Africa and Eastern Asia. So, it is clear that the major cause of death in human is considered to be liver tumor [4]. There are various signs and symptoms of liver tumor which include unexplained weight loss, swollen abdomen, yellowish skin, dark colored urine, pale colored stools, few weeks of appetite loss, feeling full even after a small meal, high temperature and sweating, vomiting and nausea. There are various risk factors that can lead to liver cancer such as Hepatitis B infection, Hepatitis C infection, excessive alcohol consumption, diabetes and obesity.

Analyzing medical images manually is very difficult due to large size of medical image database, so computer oriented surgery has become one of the major research subject [5] and this has led to medical imaging modalities such as X-ray, CT [6], Magnetic Resonance Imaging (MRI) [7, 8], SPECT [9], PET [10] and ultrasound [11, 12].

In this paper, problem of PET/CT based liver segmentation to detect liver tumor is addressed using Binary tree quantization clustering algorithm and feature extraction is performed to calculate area, perimeter and equiv-diameter of tumor detected by binary tree quantization. These are calculated to check the accuracy of our process and all the parameters of the output image are calculated and compared with the original input image. Binary tree quantization clustering algorithm is used as it directly works on the RGB image which eliminates the requirement of converting the grayscale image into colored image and so is well suited to be used for PET/CT images. Firstly image pre-processing is done to reduce the effect of noise and preserve liver tumor edges for successful segmentation. Then, Binary tree quantization clustering is applied for segmentation. After segmentation, ROI selection is done manually to calculate various features of tumor. Finally the method is compared with same features calculated for original image and traditional K-means clustering algorithm for checking the performance of our method with K-means method. The results show that the method successfully segmented tumor with accuracy compared to K-means method. In PET/CT imaging modality, within a single scanner PET and CT scans are combined and hence in a single scanning session this modality provide both

functional and anatomical imaging [13] i.e. in PET/CT, in the same session, images are acquired from both the modalities sequentially which are then combined into single superposed image. CT pictures of the body structures are taken firstly. Then at the same time, areas where cells are more active than normal cells of the body are shown up by the radioactive substance. Both the information is then combined by the scanner which allows the doctor to visualize changes in the cell's activity (if any) and know where the changes are happening exactly. The most commonly radioactive substance used is  $^{18}\text{F}$ -FDG (fluorodeoxyglucose). For carrying out the PET/CT scan, radioactive substance is injected through a small tube which is put into the veins in the back of hand or arm. The scan is carried out only when the body has absorbed the radioactive substance (it takes at least one hour) and the bladder is emptied. The patient needs to lie down on a narrow table which moves through the scanner and detector. During the scan, X-rays emitted by the CT scanner go to the detector through the patient's body to generate its anatomical structures. Then PET scanner (which is a large machine with round doughnut shaped machine in the middle similar to CT and has multiple rings of detectors), detects the radiations which are emitted from the patient because of the radioactive substance which is used by the computer to generate the cell activity (functional activity) in tissues of the body. All the cells in the body use radioactive substance (namely  $^{18}\text{F}$ -FDG) as an energy source. So, cancer cells grow more rapidly than healthy cells. This forms the image generation in PET/CT scans. Due to reduced scanning time in PET/CT, it is considered reliable in clinical practices [14].

## II. RELATED WORK

Variety of segmentation methods have been proposed for CT, MRI and PET images to detect tumor but there have been little attempts to work on PET/CT images. *Amir H. Foruzan et.al* [15] proposed a technique for segmentation of liver in CT data for liver initial border estimation in which they started with image simplification, then searched rib bones, connected them together to find ROI of liver. They then used split thresholding technique to segment the images. Different colors were assigned to objects present in ROI, the split-threshold step and the objects that were found in 75% of right part of the abdomen. After this a colored image was obtained in which liver had a specific color from where liver boundary was extracted. In the method of *Xing Zhang et.al* [16], automatic liver segmentation included average liver shape model localization in CT via 3D generalized Hough Transform, subspace initialization of Statistical Shape Model through intensity and gradient profile and then deforming the model to liver contour through optimal surface detection method based on graph theory. *Laszlo Rusko et.al* [17] method automatically segments the liver using region-growing facilitated by pre- and post-processing functions, which considers anatomical and multi-phase information to eliminate over and under-segmentation. *Hassan Masoumi et.al* [18]

extracted features of liver region in MRI images using watershed algorithm and artificial neural network leading to automatic liver segmentation. But all these methods resulted only in liver boundary and did not detect liver tumor. *O. Lezoray et.al* [19] proposed an unsupervised clustering technique in which watershed operates on distance function to centers of class for determining the number of classes. In this method, segmentation of colored image considered pairwise color projections where each of these projections is analyzed to look for the dominant colors of 2-D histogram and to fully automate the segmentation, energy function was used to quantify the quality of the segmentation. But the difficulty with the histogram method is to identify peaks and valleys in the image. *Marisol Martinez-Escobar et.al* [20] first colorized the pixels representing tumor and healthy tissues and then used threshold method for segmentation to detect tumor to overcome the problem as faced in histogram. But these methods are either performed on CT or MRI images or the images are first colored and then segmentation is applied. Since morphological changes always precede metabolic changes and are detected through imaging modalities like CT or MRI, PET is expected in enabling an early assessment of response to treatment.  $^{18}\text{F}$ -FDG PET has been reported to give earlier response for tumor detection than CT [21].

Positron emission tomography (PET) with  $^{18}\text{F}$ Fluorodeoxyglucose ( $^{18}\text{F}$ -FDG) is widely suggested method medical imaging as numerous tumors are diagnosed very accurately which has improved the decision for therapy consideration and assessing patients having cancer at different stages in the last two decades [22, 23]. It is based on the tumor specific high intracellular accumulation of the glucose analog fluorodeoxyglucose ( $^{18}\text{F}$ -FDG) [24]. It gives tumor's physiological information and its metabolic activities [25]. PET/CT provides functional and anatomical imaging within a single scanner in a single scanning session [26]. Though PET has been replaced by PET/CT, most of the segmentation work to detect tumor has been done on PET only [27-30].

*Baardwijk et. al* [31] provided the advantage of PET combined CT images for the segmentation purpose. *Potesil et. al* [32] segmented PET/CT images using initial hot spot detection and segmentation in PET for tumor structure appearance and used shape model to classify voxels in CT. *Xia et. al* [33] proposed an expectation-maximization algorithm using simulated annealing to automatically segment brain PET/CT images. But long execution times were the main drawback of this method. *Yu et. al* [34] proposed the co-registered multimodality pattern analysis segmentation system (COMPASS) to extract texture features from PET/CT and then used decision-tree based K-nearest-neighbor classifier to label each voxel as either "normal" or "abnormal" and the performance was compared with threshold methods: SUV value and signal/background ratio. *Yu et. al* [35] evaluated the effectiveness co-registered segmentation method to distinguish tumor from healthy tissue in

regions of head and neck. Most approaches use standard uptake value (SUV) to detect tumor which is a semi-quantitative normalization of FDG uptake in PET images and gives concentration of FDG in dose/gram body mass. But these approaches are basically used to evaluate the value and application of FDG PET/CT in clinical practices to detect tumors. It is clear from the literature review that most of the work is done either on CT, MRI or PET images alone. Most of the segmentation work has been done using thresholding algorithms, region-based algorithms, edge-based algorithms, watershed algorithms, fuzzy clustering based algorithms and graph-based algorithms in PET images, CT images or combined PET/CT images. But these methods have various limitations. Thresholding algorithms depend on intensity distribution of image. In PET and PET/CT images, thresholding and graph based methods are generally based on SUV values which are sensitive to volume variation in tumor or structural/functional volumes. Edge-based algorithms produce disjoint edges. Region-based algorithms require manual initialization. Watershed algorithm leads to over-segmentation and is poor in detecting thin structures in images. Graph based algorithms provide global solutions and so are computationally expensive. Fuzzy clustering based algorithms require training of the dataset and the accuracy depends on the selected training samples and therefore, these are more tedious to use. The proposed algorithm i.e. *Binary Tree Quantization Clustering Algorithm* is conceptually simple as it is based on divide and conquer rule which recursively divides the problem (image) into sub-problems where solving the sub-problems and combining their solutions give the solution to the original problem. The method makes use of binary tree structure so it reduces the computation greatly and does not lead to over-segmentation.

### III. PROPOSED WORK

Our proposed method for PET/CT-based liver segmentation to detect tumor and perform feature extraction consists of 5 steps as shown in *fig1*. The method started with reading the input image and applying the RGB median filtering which is to be done to remove noise to increase accuracy of our process. The output of median filtering process is taken as input for segmentation. Then image clustering is performed using binary tree quantization method to segment the image. In this method on the basis of the color, the clusters of pixels are computed. Then feature extraction is done for calculating area, perimeter and equiv-diameter of tumor detected by binary tree quantization. By this procedure we came to know about accuracy of our process. For this we have compared all the parameters calculated on our output image with the original input image. Finally the method is also compared with traditional K-means method.

#### A. Preprocessing

Noise in PET/CT images may be caused by variability in organ/tissue which looks like random noise. Noise can

be removed by smoothing the image with a two types of filters i.e. *low pass averaging filters* and *low pass median filters*. Low pass filtering means removing the high frequency content from the image. Noise is a high frequency component and hence low pass filtering is used to remove noise.

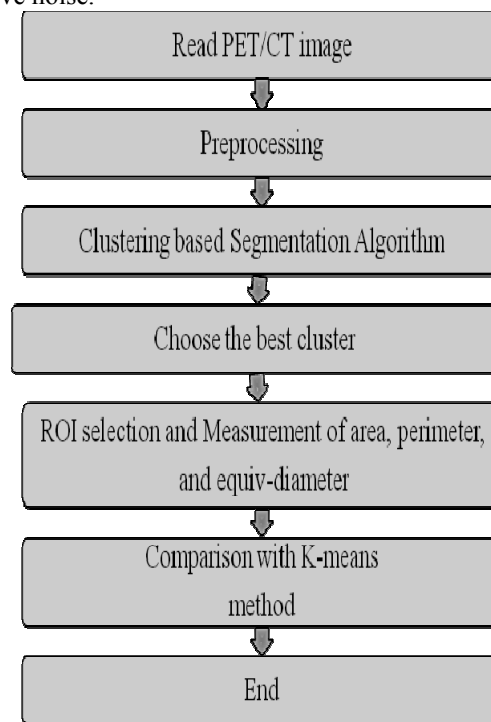


Fig 1: Flowchart of the Proposed Method

*Low pass averaging filter* is also known as linear filter where value of each pixel is replaced by the average of all the values of intensities in the neighborhood defined by the filter mask and image with reduced sharp transitions in intensities is produced. However, low pass averaging filter results in blurred edges. *Low pass median filter* is also known as non-linear filter as its response is based on the ordering of the pixels in an image, and replaces the value of a pixel by the median of the intensity values in the neighborhood of that. In our work to remove noise, we denoised the image using 2D-median filter in which depending upon the intensity, the pixels in the neighborhood window are ranked and the median (i.e. the middle value) becomes the output value for the centre pixel. The image is denoised using median filter rather than averaging filter as it removes noise without distorting the edges. This is because in median filtering, the output value is from the neighboring values, new unknown values are not created near the edges, so median filtering is more effective when our main aim is to simultaneously reduce noise and preserve the edges. To apply median filter on colored images, number of colors is firstly determined in the image and then the filter is applied on each color separately. All the denoised components are combined to get the final denoised image i.e. image is firstly converted into red, green and blue planes or constituents, median filtering is then performed on red, green and blue constituents separately and then all

the denoised RGB constituents are combined to get the final denoised image.

The output of median filtering process i.e. the denoised image is taken as input for segmentation step. Steps of median filtering are shown in fig 2:

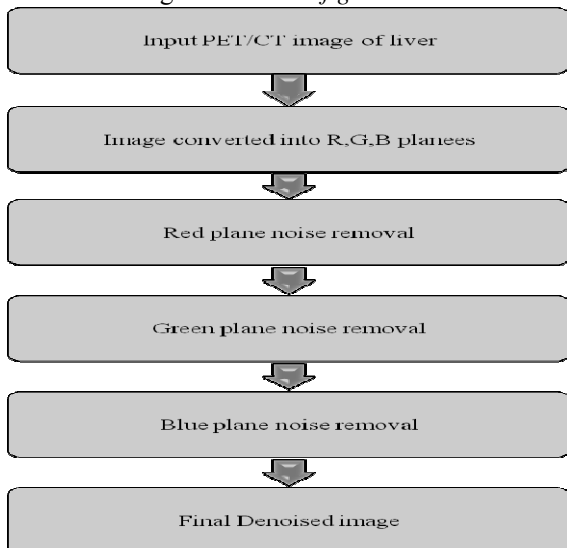


Fig 2: Flowchart of median filtering in all planes of RGB image

**B. Segmentation**

The denoised image is taken as input for segmentation. The proposed segmentation algorithm is based on binary tree quantization algorithm performed on PET/CT images. In this method on the basis of the color, the clusters of pixels are computed. The Orchard and Bauman method of binary tree is the base of this algorithm. Orchard and Bauman proposed a divisive palette generation algorithm, which uses a local optimization strategy in selecting the splitting axis (i.e. RGB co-ordinate axis of the color plane). In this method, partition with the largest eigen value is chosen to be split. Eigenvalue is the scalar which is associated with eigenvector where eigenvector is a vector that changes its magnitude but not its direction. The splitting axis is the one that passes through the centroid of all the colors in that region and must be perpendicular to the direction of the maximum total squared variation which is derived from the eigenvalue and eigenvector of the covariance matrix of the data in that particular region. The splitting of a node into two nodes is equivalent to selecting a plane which best splits the cluster's colors which can be found with principal component analysis (PCA) and it is called the principal axis or the eigenvector with largest eigenvalue. Mainly variance of the split node is reduced along the direction of principle eigenvector, so decrease in total squared error is considered to be proportional to total squared variation along the principle eigenvector. Therefore, it is best to split the node with the largest principal eigen vector. To conclude:

All the pixels are placed in the same cluster in the beginning. The cluster is then split around its mean value projection on the first principle component. The parameters to the clustering algorithm are the number of

clusters, K, to use which is set/input by the user, and the first cluster  $C_1$ .

1. Initialize the first cluster,  $C_1$
2. Calculate the mean,  $\mu_1$ , and the covariance matrix  $\Sigma_1$  of the cluster  $C_1$
3. For  $i=2$  to  $K$  do
4. Find the cluster,  $C_n$  with the largest eigenvalue and its associated eigenvector  $e_n$ .
5. Split  $C_n$  in two sets along the mean value projections on the eigenvector,  $C_i = \{x \in C_n : e_n^T x_n \leq e_n^T \mu_n\}$  and update the original cluster with other half  $C_n^* = C_n - C_i$ .
6. Compute mean and covariance matrix of the two halves obtained in step2 as  $\mu_n^*, \Sigma_n^*, \mu_i$  and  $\Sigma_i$ .

**C. ROI Selection and Shape Feature Extraction**

After segmentation, Region of interest (ROI) is selected using GUI based polygon method which selects a polygonal region of interest within an image [36]. Then shape feature extraction is performed on the selected ROI to calculate area, equiv-diameter, and perimeter of the tumor. *Area* used to calculate the actual number of pixels in the region. *Equiv-diameter* is the scalar which specifies the diameter of the region of interest. *Perimeter* gives the distance between each adjoining pair of pixels around the border of the region.

**D. K-means Clustering Method**

K-means method is a data-clustering algorithm which groups together the objects with similar characteristics to form clusters. The number of clusters (k-clusters) to be formed to classify the dataset is fixed apriori and is given as input parameter. Each object is assigned to the cluster which is close to it. The mean of the cluster is recomputed and the process is repeated again. It works as follows:

1. Cluster seeds are chosen at random initially i.e. value of k which represent “mean” of the clusters.
2. Each object is assigned to the cluster close to it based upon the Euclidean distance between the object and the cluster center. The object is assigned to the cluster with the smallest squared Euclidean distance.
3. For each cluster, new cluster center is recomputed as average of the objects/points in that cluster.
4. Step 2 and 3 are repeated until no more objects are left for assignment to the cluster i.e. until the clusters converge.

K-means method was implemented so as to compare its results with our proposed method to check accuracy.

**E. Comparison of Proposed Method with K-means Clustering Method**

The proposed method is compared with k-means method to check for accuracy of segmentation. This was

done by comparing the shape features of the proposed method with the features extracted from original image and k-means clustering method. The shape features used for comparison are area, perimeter and equiv-diameter. These shape features have been used as a measure to quantify the size of tumor which is one of the prime concerns for medical practitioners and patients.

IV. VISUAL RESULTS OF PROPOSED METHOD AND K-MEANS CLUSTERING METHOD

The binary tree quantization method was evaluated on PET/CT liver images obtained from multi-specialist hospital. We have tested our algorithm on twelve PET/CT images. The images of liver tumor were provided by a reputed hospital and no detail of the patient history was provided. Accuracy of our method is compared with traditional K-means clustering approach. Output resulting images of the proposed method on first pateint chosen at random are shown from figures 3-7 and output images of K-means method are shown in figure 8. A Visual comparison of the best image produced by the proposed method and k-mean clustering is also presented in figure 9.

1. Fig 3 shows the Original PET/CT scan image of liver tumor

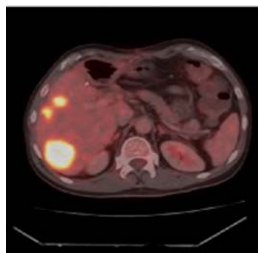


Fig 3 : Original PET/CT scan image of Patient-1

2. Fig 4 shows the Red, Green and Blue Constituents of Figure 4.1

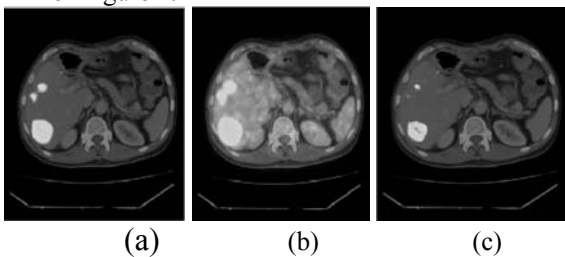


Fig 5: (a)Red Constituent; (b)Green Constituent; (c)Blue Constituent

3. Fig 6 shows the Denoised Image after Median Filtering

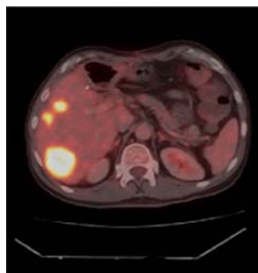


Fig 6 : Figure 4.1 after filtering

4. Fig 7 shows Output of Binary Tree Quantization Clustering Method

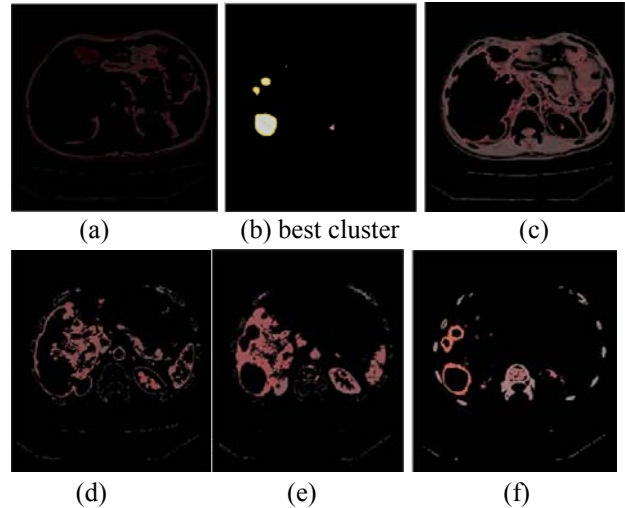


Fig 7: Clusters of Figure 4.3 after Binary Tree Quantization Clustering

Fig. 7 shows various clusters generated by binary tree quantization clustering method where (a) cluster1 roughly shows the organs except the liver; (b) cluster2 shows the brightened tumor detected by the proposed method and so, is selected as the best cluster for feature extraction; (c) cluster3 shows the organs other than liver; (d)-(e) cluster4 and 5 show liver area; (f) cluster6 shows the rough boundary of the detected tumor in liver.

5. Fig 8 shows the Output of K-means Method

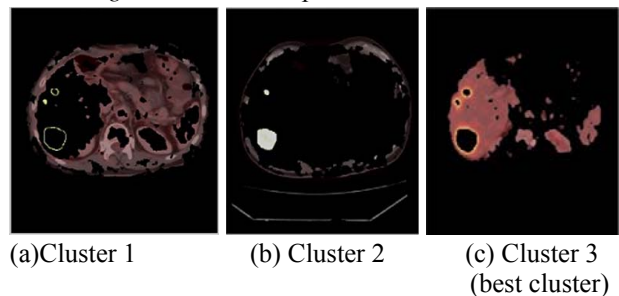


Fig. 8 shows various clusters generated by k-means clustering method where (a)-(b) cluster 1 and 2 do not show the entire tumor present in the liver; (c) cluster 3 shows the entire tumor present in the liver and so is taken as the best cluster for feature extraction.

6. Fig 9 show the visual comparison of the proposed method with k-means method

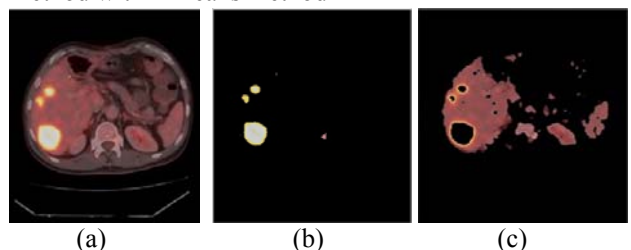


Fig 9 Visual Comparison of proposed method with k-mean clustering on Patient-1(a) Original Image (b)Best image of proposed method (c) Best image produced by k-means method.

Fig 9 draws a visual comparison of the best clusters produced by our method and k-mean clustering method. The output shows that proposed method performs better than k-mean clustering as it had detected the tumor present in the image very clearly. The size and shape of the tumour is very much similar to original PET/CT

image. Although some tiny spots other than tumor are detected but they are negligible.

From the visual results of binary tree quantization method and k-means clustering method it is clear that clusters generated by the proposed method are more accurate, clear and brighter than the clusters generated by k-means clustering method. Tumor detected in the best cluster by the proposed method is close to the tumor in original image whereas k-means method was not able to detect tumor completely or tumor detected is not clear.

V. QUANTITATIVE COMPARISON OF BINARY TREE CLUSTERING METHOD AND K-MEANS AND ORIGINAL IMAGE

To check accuracy of the proposed method, the method is compared with traditional k-means clustering method and original image by calculating shape features on the selected cluster. Shape features calculated on original image, best cluster generated by binary tree quantization method and k-means clustering are shown in section A, B and C respectively.

A. Shape Feature Results on Original Input Image

All the shape features calculated on original input image are shown in table I:

TABLE I. RESULTS ON ORIGINAL IMAGE

Images	Area	Perimeter	Equiv-diameter
Image 1	3333	514.5412	65.1437
Image 2	2527	191.9239	56.7228
Image 3	950	154.4092	34.7790
Image 4	955	132.8528	34.8704
Image 5	223	56.4264	16.8503
Image 6	493	97.3970	25.0541
Image 7	1551	203.2376	44.4387
Image 8	2822	60.526	59.9423
Image 9	3181	551.0437	63.6410
Image 10	255	60.8701	18.0188
Image 11	3770	239.9239	69.2828
Image 12	2690	325.0193	58.5236

B. Shape Feature Results on Best Cluster Generated by Binary Tree Quantization Clustering Method

After selecting the best cluster, shape features i.e. area, perimeter and equiv-diameter are calculated on ROI. This result is given in table II as:

TABLE II. RESULTS OF BINARY TREE QUANTIZATION CLUSTERING

Images	Area	Perimeter	Equiv-diameter
Image 1	3195	215.3381	63.7809

Image 2	2290	166.7107	53.9974
Image 3	873	143.9828	33.3397
Image 4	839	92.4264	32.6841
Image 5	133	33.6985	13.0131
Image 6	415	92.4264	22.9868
Image 7	1329	123.0538	41.1356
Image 8	2683	56.2843	58.4474
Image 9	2863	361.6051	60.3762
Image 10	243	59.2132	17.5897
Image 11	3743	238.9361	69.0343
Image 12	2632	304.5341	57.8893

C. Shape Feature Results on Best Cluster Generated by K-means Clustering Method

After selecting the best cluster, shape features i.e. area, perimeter and equiv-diameter are calculated on ROI. This result is given in table III as:

TABLE III. RESULTS OF K-MEANS METHOD

Images	Area	Perimeter	Equiv-diameter
Image 1	747	47.6985	30.8401
Image 2	974	70.5269	35.2156
Image 3	633	136.6102	28.3894
Image 4	750	111.2965	30.9019
Image 5	113	22.6274	11.9948
Image 6	383	81.6985	22.0828
Image 7	1095	193.8234	37.3390
Image 8	1783	23.8995	47.6465
Image 9	582	116.8112	25.9282
Image 10	146	48.1421	13.6343
Image 11	3642	232.1076	68.0965
Image 12	1546	269.8650	44.3670

D. Comparison with Original Image and K-means Method

Quantitative results obtained from binary tree quantization are compared results obtained from k-means method to check accuracy of the results with the same shape features calculated on original image. Relative accuracy of each calculated shape feature is calculated as modulus of calculated value minus original value divided by original value. This is shown in table IV:

TABLE IV:  
COMPARISON OF PROPOSED METHOD WITH K-MEANS CLUSTERING METHOD AND ORIGINAL IMAGE BASED ON SHAPE FEATURES

S.No	Images	Area	Relative Accuracy	Perimeter	Relative Accuracy	Equiv-Diameter	Relative Accuracy
1	Original	3333		514.5412		65.1437	
	Proposed	3195	0.041	215.3381	0.581	63.7809	0.020
	K-means	747	0.75	47.6985	0.907	30.8401	0.526
2	Original	2527		191.9239		56.7228	
	Proposed	2290	0.093	166.7107	0.131	53.9974	0.048
	K-means	974	0.614	70.5269	0.632	35.2156	0.379
3	Original	950		154.4092		34.7790	
	Proposed	873	0.081	143.9828	0.067	33.3397	0.041
	K-means	633	0.333	136.6102	0.115	28.3894	0.183
4	Original	955		132.8528		34.8704	
	Proposed	839	0.121	92.4264	0.304	32.6841	0.062
	K-means	750	0.214	111.2965	0.162	30.9019	0.113
5	Original	223		56.4264		16.8503	
	Proposed	133	0.403	33.6985	0.402	13.0131	0.228
	K-means	113	0.493	22.6274	0.598	11.9948	0.288
6	Original	493		97.3970		25.0541	
	Proposed	415	0.158	92.4264	0.051	22.9868	0.082
	K-means	383	0.223	81.6985	0.161	22.0828	0.118
7	Original	1551		203.2376		44.4387	
	Proposed	1329	0.143	123.0538	0.394	41.1356	0.074
	K-means	1095	0.294	193.8234	0.046	37.3390	0.159
8	Original	2822		60.5269		59.9423	
	Proposed	2683	0.049	56.2843	0.070	58.4474	0.024
	K-means	1783	0.368	23.8995	0.605	47.6465	0.205
9	Original	3181		551.0437		63.6410	
	Proposed	2863	0.099	61.6051	0.888	60.3762	0.051
	K-means	582	0.817	116.8112	0.788	25.9282	0.592
10	Original	255		60.8701		18.0188	
	Proposed	243	0.047	59.2132	0.027	17.5897	0.023
	K-means	146	0.427	48.1421	0.209	13.6343	0.243
11	Original	3770		239.9239		69.2828	
	Proposed	3743	0.007	238.9361	0.004	69.0343	0.003
	K-means	3642	0.033	232.1076	0.032	68.0965	0.017
12	Original	2690		325.0193		58.5236	
	Proposed	2632	0.021	304.5341	0.063	57.8893	0.010
	K-means	1546	0.425	269.8650	0.169	44.3670	0.236

In this paper, binary tree quantization method was implemented for segmenting PET/CT liver images so as to detect tumor. It is clear from the resulting images that the proposed method works well on segmentation of PET/CT images for tumor detection and shape feature extraction. Binary tree quantization was able to detect tumor perfectly as compared to k-means method. Shape features were calculated to calculate area, perimeter and equiv-diameter of the tumor detected by the proposed method and k-means method. The calculated shape features were compared with features extracted from original image and k-mean clustering method to check the accuracy of the proposed method. From *table IV*, it is clear that the accuracy of the proposed method is far better than the k-means method and is very near to the actual image.

## VI. CONCLUSIONS

This work has tried to segment PET/CT scan images of liver using Binary Tree Quantization clustering method

for detection of tumor in the form of best cluster. Combination of filtering technique with clustering techniques had known to be beneficial for the process of segmentation of medical images as pre-processing removed the unwanted noise from the images. Feature extraction has been done to parameterize the efficiency of the process. Our method has proved that it is better than other clustering methods in detecting tumor more accurately and precisely. Our method is semi automatic as after tumor detection for the selection of region of interest we have used manual approach. This work is significant as it can help medical practitioner in focussing to the area of tumor and making it easy for classifying tumor as benign or malignant.

The previous work has focussed on segmenattion of PET/CT images although the proposed method is generating good results for liver images the same can be extended to detect tumors in other parts of the body. Other improvements can be done in the direction of making this process fully automated which can decrease the processing time of cancer detection as well as

efficiency could be increased and be able to detect tumors in large and different image datasets.

#### ACKNOWLEDGMENT

The authors would like to thank multi-specialist hospital for providing PET/CT images that helped to complete the work successfully.

#### REFERENCES

- [1] CanLive, The Hepatobiliary, Cancers Foundation, <http://canliv.org/livercancer?gclid=CPWPIuKqrkCFa0l4g odZzIAsA>(last accessed on August 30, 2013)
- [2] National Cancer Institute, <http://www.cancer.gov/cancertopics/types/liver> last accessed on August 30, 2013.
- [3] American Cancer Society, <http://www.cancer.org/cancer/livercancer/detailedguide/liver-cancer-what-is-key-statistics> last accessed on August 30, 2013.
- [4] Cancer Research UK, <http://www.cancerresearchuk.org/cancerhelp/type/livercancer/about/symptoms-of-liver-cancer> last accessed on August 30, 2013.
- [5] Masuda, Y., Tateyama, T., Xiong, W., Zhou, J., Wakamiya, M., Kanasaki, S., Furukawa, A., and Chen, Y.W.: Liver Tumor Detection in CT images by Adaptive Contrast Enhancement and the EM/MPM Algorithm. In 18th IEEE Conference on Image Processing, pp. 1421-1424, September 2011.
- [6] Hounsfield, G.N.: Computerized Transverse Axial scanning Tomography: Part 1, Description of the System. *British Journal of Radiology* 46, 1016-1022 (1973).
- [7] Lipinski, B., Herzog, H., Kops, E.R., Oberschelp, W., Muleer-Gartner, H.W.: Expectation Maximization Reconstruction of Positron Emission Tomography Images using Anatomical magnetic Resonance Information", *IEEE Transaction on Medical Imaging*, Vol. 16, pp. 129-136, April 1997.
- [8] Bazille, A., Guttman, M.A., Mcveigh, E.R., Zerhouni, E.A.: Impact of Semi-automated versus Manual Image Segmentation Errors on Myocardial Strain Calculation by Magnetic Resonance Tagging. *Investigative radiology* 29, 427-433 (1994).
- [9] Anger, H.: Use of Gamma-Ray Pinhole Camera for viva studies. *A Nature Conference on Nuclear Reprogramming and the Cancer Genome* 170, pp. 200-204, August 1952.
- [10] Ouyang, X., Wang, W.H., Johnson, V.E., Hu, X., Chen, C.T.: Incorporation of Correlated Structural Images in PET Image Reconstruction. *IEEE Transactions on Medical Imaging*, Vol. 13, pp. 627-640, August 2002.
- [11] Akgul, Y.S., Kambhamettu, C., Stone, M.: Extraction and Tracking of the Tongue Surface from Ultrasound Image Sequences. In 1998 IEEE Computer Society Conference on Computer Vision Pattern Recognition, pp. 298-303, June 1998.
- [12] Abeyratne, U.R., Petropulu, A.P., Reid, J. M.: On modeling the Tissue Response from Ultrasonic B-scan. *IEEE Transactions on Medical Imaging*, Vol. 2, pp. 479-490, August 1996.
- [13] Thomas Beyer, David W. Townsend, Tony Brun, Paul E. Kinahan, Martin Charron, Raymond Roddy, Jeff Jerin, John Young, Larry Byars and Rnald Nutt, "A Combined PET/CT Scanner for Clinical Oncology", *Journal of Nuclear Medicine*, Vol. 41, pp. 1369-1379, August 2000.
- [14] Bingsheng Huang, Martin Wai-Ming Law and Pek-Lan Khong, "Whole-Body PET/CT Scanning: Estimation of Radiation Dose and Cancer Risk", *Radiology, Medical Physics*, Vol. 251, pp. 166-174, April 2009.
- [15] Foruzan, A.H., Zoroofi, R.A., Hori, M., and Sato, Y.: A Knowledge-based Technique for Liver Segmentation in CT Data. *Computerized Medical Imaging and Graphics*, Elsevier, Vol.33, pp. 567-587, March 2009
- [16] Zhang, X., Tian, J., Deng, K., Yongfang, W., and Xiuli, I.: Automatic Liver Segmentation Using a Statistical Shape Model With Optimal Surface Detection. *IEEE Transactions on Biomedical Engineering*, Vol. 57, pp. 2622-2626, October 2010.
- [17] Rusko, L., Bekes, G., and Fidrich, M.A.: Automatic Segmentation of the Liver from Multi- and Single-Phase Contrast-Enhanced CT. *Medical Image Analysis*, Elsevier, Vol. 13, pp. 871-882, July 2009
- [18] Masoumi, H., Behrad, A., Pourmina, M.A., and Roosta, A.: Automatic liver segmentation in MRI Images using an Iterative Watershed Algorithm and Artificial Neural Network. *Biomedical Signal Processing and Control*, Elsevier, Vol. 7, pp. 429-437, February 2012
- [19] Lezoray, O. and Charrier, C.: Color Image Segmentation using Morphological Clustering and Fusion with Automatic Scale Selection. *Pattern Recognition Letters*, Elsevier, Vol. 30, pp. 397-406, March 2009
- [20] Escobar, M.M., Foo, J.L., and Winer, E.: Colorization of CT images to Improve Tissue Contrast for Tumor Segmentation. *Computers in Biology and Medicine*, Elsevier, Vol. 42, pp. 1170-1178, September 2012.
- [21] Necib, H., Garcia, C., Wagner, A., Vanderleinden, B., Emonts, P., Hendlisz, A., Flamen, P. and Buvat, I.: Detection and Characterization of Tumor Changes in 18F-FDG Patient Monitoring using Parametric Imaging. *J. of Nucl. Med.* 52, 354-361 (2011).
- [22] Lartizien, C., Francisco, S.M. and Prost, R.: Automatic Detection of Lung and Liver Lesions in 3-D Positron Emission Tomography Images: A Pilot Study. *IEEE Transactions on Nuclear Science*, Vol. 59, pp. 102-112, February 2012.
- [23] Changyang, L., Wanga, X., Xiaa, Y., Eberlb, S., Yinc, Y. and Feng, D.D.: Automated PET-guided Liver Segmentation from Low-Contrast CT Volumes using Probabilistic Atlas. *Computer Methods and Programs in Biomedicine*, Elsevier, Vol. 107, pp. 164-174, July 2011.
- [24] Blechacz, B., and Gores, G.J.: PET scan for Hepatic Mass. *Hepatology*, Vol. 52, pp. 2186-2191, December 2010.
- [25] Ming, X., Feng, Y., Guo, Y. and Yang, C.: A New Automatic Segmentation Method for Lung Tumor Based on SUV threshold on 18F-FDG PET images. In 2012 IEEE International Conference on Virtual Environments Human-Computer Interfaces and Measurement Systems (VECIMS), pp. 5-8, July 2012.
- [26] Yong, X., Stefan, E., Lingfeng, W., Michael, F., and David, D.D.: Dual-Modality brain PET-CT image segmentation based on adaptive use of functional and anatomical information. *Computerized Medical Imaging and Graphics*, Elsevier, Vol. 36, pp. 47-53, June 2011.
- [27] Belhassen, S., and Zaidi, H.: A Novel Fuzzy C-means Algorithm for Unsupervised Heterogeneous Tumor Quantification in PET. *Medical Physics*, Vol. 37, pp. 1309-1324, March 2010.
- [28] Geets, X., Lee, J.A., Bol, A., Lonneux, M. and Gregoire, V.: A gradient-based method for segmenting FDG-PET images: methodology and validation. *Eur. J. of Nucl. Med. Mol Imaging*, Springer 34, 1427-1438 (2007).

- [29] Hatt, M., Rest, C.L., Turzo, A., Roux, C., and Visvikis, D.: Fuzzy Logically Adaptive Bayesian Segmentation Approach for Volume Determination in PET. *IEEE Transactions on Medical Imaging*, Vol. 28, pp. 881-893, January 2009.
- [30] Li, H., Thorstad, W.L., Biehl, K.J., Laforest, R., Su, Y., Shoghi, K.I., Donnelly, E.D., Low, D.A. and Lu, W.: A Novel PET Tumor Delineation Method based on Adaptive region-Growing and Dual-Front Active Contours. *Medical Physics*, Vol. 35, pp. 3711-3721, August 2008.
- [31] Baardwijk, A., Bosmans, G., Boersma, L.: PET-CT based Auto-contouring in Non-Small-Cell Lung Cancer correlates with Pathology and reduces Interobserver Variability in the Delineation of the Primary Tumor and involved Nodal Volumes. *International Journal of Radiation and Oncology, Biology and Physics*, Elsevier, Vol. 68, pp. 771-778 July 2007.
- [32] Potesil, V., Huang, X., Zhou, X.: Automated Tumor Delineation using Joint PET/CT information. In: *Proc. SPIE International Symposium on Medical Imaging: Computer-Aided Diagnosis*, Vol. 65142, March 2007.
- [33] Xia, Y., Wen, L., Eberl, S., Fulham, M., Fend, D.: Segmentation of Dual Modality Brain PET/CT images using MAP-MRF model. In *2008 IEEE 10th Workshop on Multimedia Signal Processing*, pp. 107-110, October 2008.
- [34] Yu, H., Caldwell, C., Mah, K.: Automated Radiation targeting in head-and-neck cancer using Region-based Texture Analysis of PET and CT images. *International Journal of Radiation and Oncology, Biology and Physics*, Elsevier, Vol. 75, pp. 618-625, October 2009.
- [35] Yu, H., Caldwell, C., Mah, K., Mozeg, D.: Coregistered FDG PET/CT-based Textural Characterization of Head and Neck Cancer for Radiation Treatment Planning. *IEEE Transactions on Medical Imaging*, Vol. 28, pp. 374-383, February 2009.
- [36] Baisa L. Gunjal, and Suresh N. Mali, "ROI Based Embedded Watermarking of Medical Images for Secured Communication in Telemedicine", *International Journal of Computer and Communication Engineering*, Vol. 6, pp. 815-820 May 2012.